Applied Physics
Express

The Japan Society
of Applied Physics

LETTER • OPEN ACCESS

Distinguishing the EH_1 and S_1 defects in n-type 4H-SiC by Laplace DLTS

To cite this article: Tihomir Knežević *et al* 2022 *Appl. Phys. Express* **15** 101002

View the article online for updates and enhancements.

You may also like

- Defects in low-energy electron-irradiated n-type 4H-SiC
F C Beyer, C Hemmingsson, H Pedersen et al.

- Investigation of defects in 3C-SiC using deep level transient spectroscopy
P U Feiler, T Mchedlidze, K Cherkaoui et al.

- Defects evolution in n-type 4H-SiC induced by electron irradiation and annealing
Huifan Xiong, Xuesong Lu, Xu Gao et al.

This content was downloaded from IP address 93.138.131.52 on 10/06/2026 at 10:40

OPEN ACCESS
Applied Physics Express 15, 101002 (2022)
https://doi.org/10.35848/1882-0786/ac8f83

LETTER

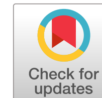

Distinguishing the EH_1 and S_1 defects in n-type 4H-SiC by Laplace DLTS

Tihomir Knežević[1], Tomislav Brodar[1], Vladimir Radulović[2], Luka Snoj[2], Takahiro Makino[3], and Ivana Capan[1*]

[1]Ruđer Bošković Institute, Bijenička 54, 10 000 Zagreb, Croatia
[2]Jožef Stefan Institute, Jamova 31, 1000 Ljubljana, Slovenia
[3]National Institutes for Quantum Science and Technology, 1233 Watanuki, Takasaki, Japan

*E-mail: capan@irb.hr

Received August 24, 2022; revised August 30, 2022; accepted September 4, 2022; published online September 09, 2022

We report on the low-energy electron and fast neutron irradiated 4H-SiC studied by deep-level transient spectroscopy (DLTS) and Laplace DLTS. Irradiations introduced two defects, E_c−0.4 eV and E_c−0.7 eV. They were previously assigned to carbon interstitial (C_i) labeled as $EH_{1/3}$ and silicon-vacancy (V_{Si}) labeled as $S_{1/2}$, for the low-energy electron and fast neutron irradiation, respectively. This work demonstrates how Laplace DLTS can be used as a useful tool for distinguishing the EH_1 and S_1 defects. We show that EH_1 consists of a single emission line arising from the $C_i(h)$, while S_1 has two emission lines arising from the $V_{Si}(h)$ and $V_{Si}(k)$ lattice sites. © 2022 The Author(s). Published on behalf of The Japan Society of Applied Physics by IOP Publishing Ltd

Electrically active radiation-induced defects in 4H-SiC have been extensively studied for decades. A whole variety of electrically active defects introduced by different radiation sources such as protons, electrons, neutrons, and ions have been revealed. Among them, two electrically active defects with deep levels at E_c−0.4 eV and E_c−0.7 eV in n-type 4H-SiC material have captivated special attention in the SiC community. They are peculiar as they always occur together, and independently of the radiation source.[1–12] Not until recently, they were commonly assigned to the same defect. However, the origin of these two radiation-induced defects has finally been elucidated.

Alfieri and Mihaila[3] reported the isothermal annealing study of the low energy (116 keV) electron radiation-induced defects in n-type 4H-SiC. They demonstrated beyond doubt that EH_1 (E_c−0.4 eV) and EH_3 (E_c−0.7 eV) are two different charge states of the same defect, and whose origin is related to a carbon interstitial (C_i). Moreover, they highlighted that $EH_{1/3}$ are not the same as S_1 (E_c−0.4 eV) and S_2 (E_c−0.4 eV). The $EH_{1/3}$ radiation-induced defects are introduced exclusively in the case of low-energy electron irradiation (<200 keV), since the silicon atoms cannot be displaced under such conditions.[3]

Outstanding progress in understanding S_1 and S_2 defects in proton irradiated 4H-SiC was made by Bathen et al.[12] They identified S_1 and S_2 as silicon-vacancy V_{si} (−3/=) and V_{Si} (=/−) charge state transitions by combining photoluminescence (PL), DLTS, and hybrid density functional theory (DFT) calculations.

Although the origin of the EH_1/S_1 (E_c−0.4 eV) and EH_3/S_2 (E_c−0.7 eV) defects has now been resolved, they still cause some confusion in the analysis of DLTS data. The reason for this is the following: DLTS signals arising from the EH_1 and S_1, as well as signals from the EH_3 and S_2, are identical in the DLTS spectra and cannot be resolved.

Since its first demonstration in 1974, DLTS has proven to be the most sensitive technique for measuring electrically active defects in semiconductors, as it can detect defects at concentrations of about 10^{10} cm^{-3}.[13,14] The main shortcoming lies in energy resolution. Two closely spaced deep energy levels cannot be resolved. However, Laplace DLTS, an isothermal technique that provides a spectral plot of a processed capacitance signal as a function of emission rate rather than temperature, gives an order of magnitude better energy resolution.[13,14]

Laplace DLTS has already proven to be a very useful technique for resolving the overlapping DLTS signals in 4H-SiC material. Here we will briefly describe the most significant examples. Alfieri and Kimoto[15] have successfully applied Laplace DLTS to resolve the overlapping emission rates of the EH_6 and EH_7, which constitute the $EH_{6/7}$ peak in the DLTS spectrum. Following the results presented by Hemingsson et al.[16] in their pioneering work on $Z_{1/2}$, Capan et al.[17] have provided conclusive evidence that the most dominant DLTS peak, known as $Z_{1/2}$, consists of two emission lines, Z_1 and Z_2. These are assigned to the $-h$ and $-k$ configurations of the carbon vacancy (V_C).[17,18] A more recent example is the work of Bathen et al.[12] on proton irradiated 4H-SiC and S_1/S_2 defects. Using Laplace DLTS, they resolved two emission lines arising from the S_1 and assigned them to the h and k configurations of the V_{si}(−3/=).

The main aim of this work is to demonstrate how Laplace DLTS can be used for distinguishing the EH_1 (E_c−0.4 eV) and S_1 (E_c−0.4 eV) defects in n-type 4H-SiC irradiated with low-energy electrons and fast neutrons.

We used n-type nitrogen-doped 4H-SiC epitaxial layers, 25 μm thick. The SiC epilayers were grown on an 8° off-cut silicon face of a 350 μm thick 4H-SiC (0001) wafer without a buffer layer.[19] The Schottky barrier diodes (SBDs) were formed by thermal evaporation of nickel through a metal mask (100 nm), while the Ohmic contacts were formed on the backside of the SiC substrate by nickel sintering at 950 °C in an Ar atmosphere.

All irradiations were performed after the SBDs fabrication, through the nickel contact and at RT. Electron irradiation was performed at Nissin Electric Group (NEG), Kyoto, Japan. The electron energy was 150 keV, and the total fluence was 1×10^{15} cm^{-2}. Neutron irradiation was performed at the Jozef Stefan Institute (JSI) TRIGA Mark II reactor, Ljubljana, Slovenia. The neutron fluence was 1×10^{13} cm^{-2}. Thermal neutrons with energy less than 0.55 eV were filtered by a cadmium box with a wall thickness

Content from this work may be used under the terms of the Creative Commons Attribution 4.0 license. Any further distribution of this work must maintain attribution to the author(s) and the title of the work, journal citation and DOI.
© 2022 The Author(s). Published on behalf of The Japan Society of Applied Physics by IOP Publishing Ltd

of 1 mm. More details on neutron irradiation are given elsewhere.[20,21]

DLTS measurements were performed using a Boonton 7200 capacitance meter (Boonton Electronics, New Jersey, USA) and an NI PCI-6521 data acquisition device (NI, Austin, USA). DLTS measurements were carried out in the temperature range of 120–380 K with a temperature ramp rate of 2 K min^{-1}. Reverse voltage, pulse voltage, and pulse width were $V_R = -10$ V, $V_P = 0$ V, and $t_P = 10$ ms, respectively. For the Laplace DLTS measurements the following acquisition settings were used: the number of samples 3×10^4, the sampling rate 10–80 kHz, and the number of averaged scans 100–800.

Figure 1 shows an as-grown 4H-SiC sample. As expected, only one DLTS peak is detected in the as-grown n-type 4H-SiC material. This is a widely known $Z_{1/2}$, with the activation energy for electron emission of 0.67 eV. It is the scrutinized defect in 4H-SiC, earlier assigned to the carbon vacancy (V_C).[22,23]

Figure 2 shows DLTS spectra for n-type 4H-SiC samples irradiated with low-energy electrons and fast neutrons.

In addition to $Z_{1/2}$, two deep-level defects at $E_c-0.4$ eV (EH_1/S_1) and $E_c-0.7$ eV (EH_3/S_2) are detected in irradiated 4H-SiC samples. As previously described in the text, these traps were assigned to the Ci-related defects (EH_1 in the low energy electron irradiated samples) and V_{si} (S_1 in the fast neutron irradiated samples). An interesting feature has been observed in Fig. 2. While the ratio between EH_1:EH_3 is 1:1, introduction rates for S_1 and S_2 significantly differ.

This brings us to the main objective of this work. How can we distinguish the E_c–0.4 eV level in the low energy electron (EH_1) or fast neutron (S_1) irradiated 4H-SiC samples? Following the examples of successful application of the Laplace DLTS technique, we have applied Laplace DLTS to make further progress in understanding EH_1 and S_1 defects.

Figure 3 shows Laplace DLTS measurements at different temperatures for the low-energy electron irradiated 4H-SiC sample.

Laplace DLTS measurements of EH1 reveal a single emission line (Fig. 3). The estimated activation energy is 0.40 eV. As already proposed by Alfieri and Mihaila[3] EH_1 is

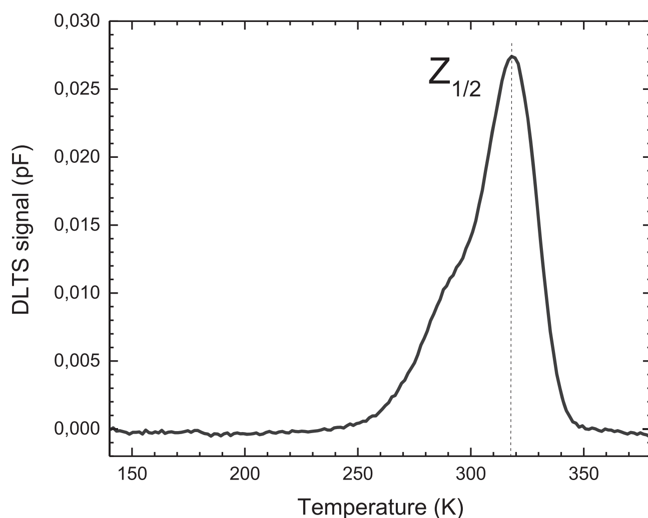

Fig. 1. DLTS spectrum for the as-grown 4H-SiC sample.

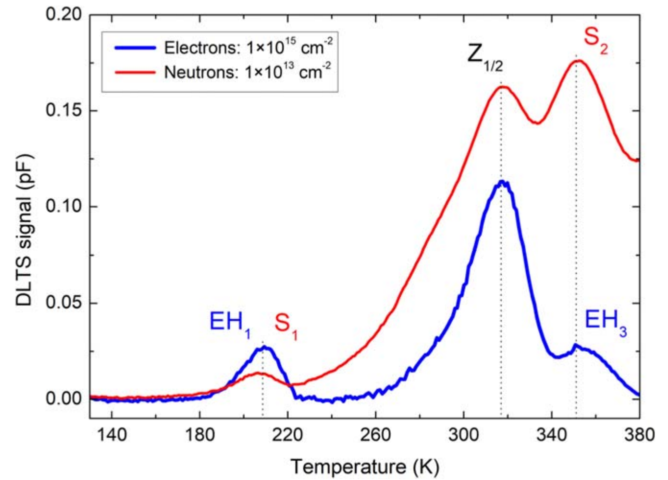

Fig. 2. (Color online) DLTS spectra for the 4H-SiC samples irradiated with low-energy electrons and neutrons.

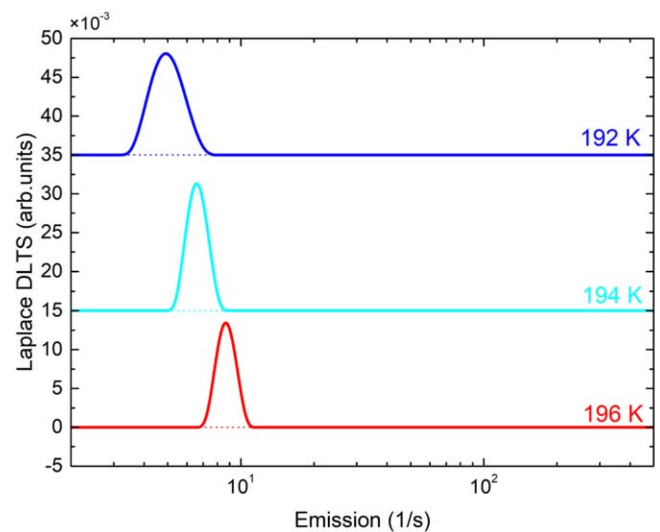

Fig. 3. (Color online) Laplace DLTS spectra measured at selected temperatures for the low-energy electron irradiated 4H-SiC.

assigned to C_i related defect. Recently, Coutinho et al.[24] have assigned the metastable defect, known as M-center,[25,26] to carbon interstitials. Combining the DFT calculations and isothermal DLTS measurements, they show that M_1 ($E_c-0.42$ eV), one of four defects arising from the M-center, is C_i located at the hexagonal lattice site, $C_i(h)$. Additional attempts in solving the puzzle related to Ci-related defects were done by Karsthof et al.[27] Knezevic et al.[28] have applied DLTS and Laplace DLTS for studying the metastable defects in low-energy electron irradiated 4H-SiC and concluded that M_1 is in fact identical to EH_1. We, therefore, assign EH_1 (shown in Fig. 3) to $C_i(h)$.

Figure 4 shows Laplace DLTS measurements for S_1 at different temperatures. Laplace DLTS measurements reveal that S_1 consists of two emission lines, with activation energies of 0.40 and 0.41 eV. They are assigned to V_{Si} at $-h$ and $-k$ lattice sites. This is consistent with the previously published work done by Bathen et al.[12]

The difference between the results obtained by Bathen in the proton irradiated 4H-SiC samples, and those presented here (fast neutron irradiated) is in the ratio between two emission lines arising from the S_1. While in the proton

© 2022 The Author(s). Published on behalf of The Japan Society of Applied Physics by IOP Publishing Ltd

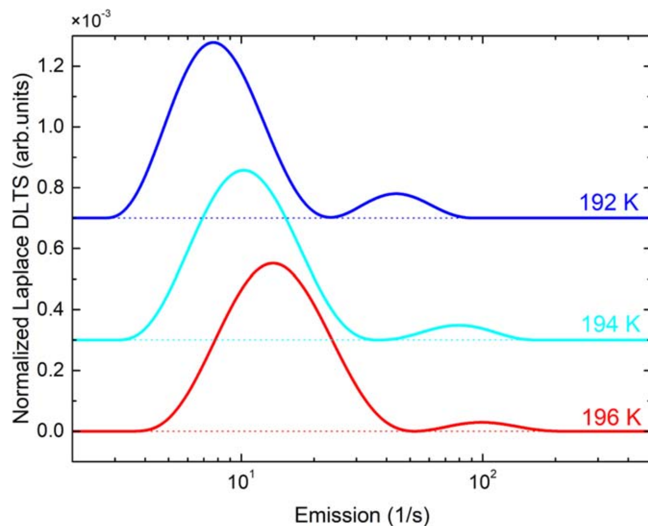

Fig. 4. (Color online) Laplace DLTS spectra measured at selected temperatures for the fast neutron irradiated 4H-SiC.

irradiated samples the ratio is close to 1:1, in our case the ratio is around 1:6. The ratio shows the occupancy of the $-h$ and $-k$ lattice sites, and it indicates that the $-h$ sites are more favorable than the $-k$ sites (for the neutron irradiated samples). The explanation for this difference is most likely due to the different sample preparations. In the proton irradiated study, the 4H-SiC samples were annealed upon irradiation, and thermal equilibrium between $-h$ and $-k$ sites was reached. In our case, no thermal annealing was performed upon the fast neutron irradiation.

Laplace DLTS has provided indisputable evidence that EH_1 and S_1 originate from different defects. Moreover, it provides direct evidence that EH_1 consists of a single emission line arising from the C_i at the $-h$ lattice site, in contrast to S_1 which has two emission lines arising from the V_{Si} at the $-h$ and $-k$ lattice sites. Therefore, Laplace DLTS can be used for easy and conclusive discrimination of the EH_1 and S_1 defects in n-type 4H-SiC material.

Acknowledgments This work was supported by the North Atlantic Treaty Organization Science for Peace and Security Program through Project No. G5674.

ORCID iDs Ivana Capan https://orcid.org/0000-0002-8550-6451

1) F. C. Beyer, C. Hemmingsson, H. Pedersen, A. Henry, E. Janzén, J. Isoya, N. Morishita, and T. Ohshima, J. Appl. Phys. **109**, 103703 (2011).
2) G. Alfieri, E. V. Monakhov, B. G. Svensson, and M. K. Linnarsson, J. Appl. Phys. **98**, 043518 (2005).
3) G. Alfieri and A. Mihaila, J. Phys.:Condens. Matter **32**, 465703 (2020).
4) M. L. David, G. Alfieri, E. M. Monakhov, A. Hallén, C. Blanchard, B. G. Svensson, and J. F. Barbot, J. Appl. Phys. **95**, 4728 (2004).
5) D. M. Martin, H. Kortegaard Nielsen, P. Lévêque, A. Hallén, G. Alfieri, and B. G. Svensson, Appl. Phys. Lett. **84**, 1704 (2004).
6) A. T. Paradzah, F. D. Auret, M. J. Legodi, E. Omotoso, and M. Diale, Nucl. Instrum. Methods Phys. Res. B **358**, 112 (2015).
7) E. Omotoso, W. E. Meyer, F. D. Auret, A. T. Paradzah, and M. J. Legodi, Nucl. Instrum. Methods Phys. Res. B **372**, 312 (2016).
8) A. Castaldini, A. Cavallini, L. Rigutti, F. Nava, S. Ferrero, and F. Giorgis, J. Appl. Phys. **98**, 053706 (2005).
9) T. Brodar, L. Bakrač, I. Capan, T. Ohshima, L. Snoj, V. Radulović, and Ž. Pastuović, Crystals **10**, 845 (2020).
10) R. Karsthof, M. F. Bathen, A. Galeckas, and L. Vines, Phys. Rev. B **102**, 184111 (2020).
11) Z. Pastuović, R. Siegele, I. Capan, T. Brodar, S. Sato, and T. Ohshima, J. Phys.:Condens. Matter **29**, 475701 (2017).
12) M. E. Bathen, A. Galeckas, J. Müting, H. M. Ayedh, U. Grossner, J. Coutinho, Y. K. Frodason, and L. Vines, npj Quantum Inf. **5**, 111 (2019).
13) L. Dobaczewski, A. R. Peaker, and K. B. Nielsen, J. Appl. Phys. **96**, 4689 (2004).
14) I. Capan and T. Brodar, Electron. Mater. **3**, 115 (2022).
15) G. Alfieri and T. Kimoto, Appl. Phys. Lett. **102**, 152108 (2013).
16) C. G. Hemmingsson, N. T. Son, A. Ellison, J. Zhang, and E. Janzén, Phys. Rev. B **58**, R10119 (1998).
17) I. Capan et al., J. Appl. Phys. **123**, 161597 (2018).
18) I. Capan, T. Brodar, J. Coutinho, T. Ohshima, V. P. Markevich, and A. R. Peaker, J. Appl. Phys. **124**, 245701 (2018).
19) M. Ito, L. Storasta, and H. Tsuchida, Appl. Phys. Express **1**, 015001 (2008).
20) I. Capan, T. Brodar, Y. Yamazaki, Y. Oki, T. Ohshima, Y. Chiba, Y. Hijikata, L. Snoj, and V. Radulović, Nucl. Instrum. Methods Phys. Res. B **478**, 224 (2020).
21) I. Capan, T. Brodar, T. Makino, V. Radulovic, and L. Snoj, Crystals **11**, 1404 (2021).
22) N. T. Son et al., Phys. Rev. Lett. **109**, 187603 (2012).
23) I. Capan, Y. Yamazaki, Y. Oki, T. Brodar, T. Makino, and T. Ohshima, Crystals **9**, 328 (2019).
24) J. Coutinho, J. D. Gouveia, T. Makino, T. Ohshima, Ž. Pastuović, L. Bakrač, T. Brodar, and I. Capan, Phys. Rev. B **103**, L180102 (2021).
25) H. K. Nielsen, A. Hallén, D. M. Martin, and B. G. Svensson, Mater. Sci. Forum **483–485**, 497 (2005).
26) H. K. Nielsen, A. Hallén, and B. G. Svensson, Phys. Rev. B **72**, 085208 (2005).
27) R. Karsthof, M. E. Bathen, A. Kuznetsov, and L. Vines, J. Appl. Phys. **131**, 035702 (2022).
28) T. Knežević, A. Hadžipašić, T. Ohshima, T. Makino, and I. Capan, Appl. Phys. Lett. **120**, 252101 (2022).

© 2022 The Author(s). Published on behalf of The Japan Society of Applied Physics by IOP Publishing Ltd